Numerical Study of Copper Antimony Sulphide ($CuSbS_2$) Solar cell by SCAPS-1D

Nancy Obare[1], Wycliffe Isoe[1], Amos Nalianya[1] Maxwell Mageto[1,2] and Victor Odari[1,2]

1. Department of Physics, Masinde Muliro University of Science and Technology, P.O Box 190-50100, Kakamega, Kenya.

2. Materials Research Society of Kenya, P.O. Box 15653-00503 Nairobi, Kenya.

Corresponding author: nancymoraamonantia@gmail.com

Abstract

Copper antimony sulphide has ability in applications on photovoltaics since it is a promising, less toxic, earth abundant absorber material. In this study, the photovoltaic characteristics of copper antimony sulphide ($CuSbS_2$) photovoltaic cell were simulated and studied by one dimensional solar cell capacitance simulator (SCAPS-1D) to improve their operations. This study investigated the impact of modifying the thicknesses of fluorine-doped tin oxide (FTO), cadmium sulphide (CdS), carbon(C), and $CuSbS_2$ absorber layer, Also the amount of doping and the number of defects on $CuSbS_2$ photoactive layer, the structure of the solar cell is made up of glass, FTO, n-CdS, p-$CuSbS_2$, C, and Au. The optimum parameters of the designed photovoltaic cell yielded 0.9388 V of open-circuit voltage (V_{oc}), the short-circuit current density (J_{sc}) was 28.31 mA/cm^2, the fill factor (FF) of 60.8%, and the solar cell efficiency of 16.17%. The ideal thickness was discovered to be 300 nm for the $CuSbS_2$ solar cell. The defect density increment led to a decrease in carrier lifetime resulting also to decrease in diffusion length and the optimum absorber layer doping concentration was found to be 10^{18} cm^{-3}.

Keywords: $CuSbS_2$, SCAPS-1D, thin film, simulation,efficiency.

1. Introduction

Researchers have focused a lot of interest on chalcogenide-based thin films because they have seen it as a potentially useful material for photovoltaics. The maximum efficiency of thin films photovoltaic cells using chalcogenide absorber materials, like cadmium telluride (CdTe) and copper indium gallium selenide (CIGS), are 22.9% and 23.3%, respectively (Ghorbani, 2020). The production of these solar cells has been hampered, by the harmful nature of cadmium and the costly indium, telluride, and gallium (Benami, 2019). $CuSbS_2$ is a ternary layered semiconductor material with minimal toxicity, highly absorption coefficient of around 10^6 cm^{-1}, and an optical bandgap of roughly 1.5 eV, making it a promising option for environmentally friendly and commercially viable photovoltaics (Rabhi et al., 2008). $CuSbS_2$ photovoltaic cells have been subject of a number of studies. A photovoltaic cell with a conversion efficiency of 3.13% was fabricated by electroplating Cu/Sb stacked layers and then sulphurizing them at 45 °C in H_2S gas for 30 minutes (Septina et al., 2014). Yang et al., (2014) also revealed $CuSbS_2$ thin film, which were produced via spin coating CuSbS stock solution on fluorine doped tin oxide coated substrate and achieving an efficiency of 0.5%. However, by simulating the material using the solar cell configuration FTO/CuSbS2/CdS/ZnO/ZnO:Al/Au, they found that the efficiency was poor due to the low open voltage brought on by significant recombination losses at the interface between CdS and $CuSbS_2$. Macías et al., (2017) found that the solar cell structure of SnO2:F/CdS/Sb2S3/CuSbS2/C:Ag has an efficiency of 0.66%as a result of low V_{oc}. Olopade et al., (2018) used SCAPS-1D to model and simulate copper antimony solar cell by varying buffer layer made of CdS, InS, ZnSe, and ZnS. From the simulation, they reported efficiency of 3.78% of the solar cell structure ZnO: Al/CdS/$CuSbS_2$/Mo. By optimizing indium sulphide buffer layer, the efficiency improved to 3.88% indicating that, it was an appropriate buffer layer although the cost of indium which is relatively expensive limits its use. The effect of low open circuit voltage is the major challenge hindering efficiency the solar cell(Wang et al., 2021).Also by considering the solar cell structure In_2S_3/CdS/$CuSbS_2$/Mo, an efficiency of 2.99% was attained which is due to cliff-like conduction band(Ghorbani, 2020). Sadanand & Dwivedi,(2020) did comparison study between CZTS, $CuSbS_2$ and $CuSbSe_2$ using solar cell architecture ITO/ZnS/$CuSbS_2$/Mo and from their research they obtained an efficiency of 17.3% while using $CuSbS_2$ as absorber layer, indicating a promising result for an alternative material which is relatively cheap, earth abundant, less toxic(Xu et al., 2018) and has a high potential for photovoltaic applications. In device fabrication of solar cells, the choice of material for each layer, has an effect on the operations of the cell. Therefore, this paper reports on numerical simulation of $CuSbS_2$ solar cell with the structure glass /FTO/n-CdS/p-$CuSbS_2$/C/Au by one dimensional solar capacitance simulator software invented by the University of Gent (Burgelman et al., 2000). Buffer layer thickness of different material was varied, dopant concentration and defect density have been also varied for an optimum and realistic performance of the solar cells that has ability to substitute Silicon based photovoltaic cells whose prospect has been hindered by energy loss through heat production.

2. Materials and methods

In this study, $CuSbS_2$ was employed as an absorber material in the solar cell construction glass/FTO/n-CdS/p-$CuSbB_2$/C/Au in order to investigate its optoelectronic properties and photovoltaic applicability. ETL and HTL have been implemented using CdS and C, respectively. As a cathode, the back contact of gold with a work function of 5.1eV was utilized. All simulations were performed at a constant 300K temperature, 1000W/m^2 incident power, and AM 1.5G spectrum. Numerous faults may be present at the interface (Perniu et al., 2006)(Willian de Souza Lucas et al., 2017) In order to explore recombination and its effect on solar cell performance, we constructed a single level (neutral) defect mechanism with an energy distribution of 0.6eV above the greatest EV, which is like the work presented by Nalianya et al., (2021)

1.1*Material Parameters and simulator Model for the $CuSbS_2$ photovoltaic Cell.*

SCAPS-1D version 3.3.07 was used to predict the structure and characterization of $CuSbS_2$. ("SCAPS3307")(Burgelman et al., 2000). Structure of photovoltaic cell was FTO/CdS (ETL)/$CuSbS_2$ (absorber)/C (HTL)/Au (back contact), with neutral defect layers at the CdS/$CuSbS_2$ and $CuSbS_2$/C interfaces, as shown in Figure 1. It's crucial for the photovoltaic cell's performance that each layer of the solar cell's structure is in place. The n-type material fluorine-doped tin oxide, which has a work function of 4.4 eV and a bandgap of 3.5 eV, was the material of choice for the anode (front contact). To avoid a short circuit at the front contact, cadmium sulfide was utilized as an electron transport layer. FTO was chosen over ITO due to its superior chemical inertness, stability under heat, hard mechanicalness, strong conductivity, low cost, and constant sheet resistance throughout sintering (Andersson et al., 1998). Also, tin oxide coatings are exceptionally transparent in the visible spectrum. Parameters for the simulation layer are shown in Table 1 below, which were derived from the literature, (Banu et al., 2019)

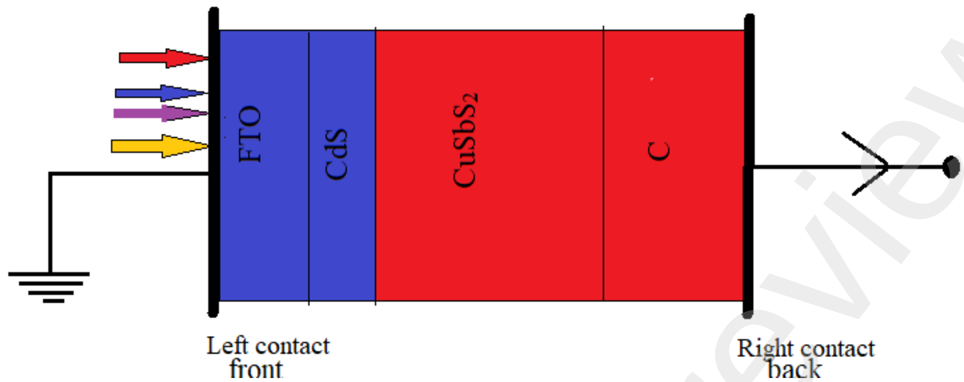

Fig.1. $CuSbS_2$ solar cell structure.

Table 1. Simulation Parameters of $CuSbS_2$ photovoltaic cell

Solar cell parameters	FTO	$CuSbS_2$	CdS	C
Bandgap, E_g (eV)	3.5	1.5	2.42	3
Thickness, d (µm)	0.1(varied)	0.3(varied)	0.01	0.35
Electron affinity, χe (eV)	4	3.85	4.5	2.45
Relative dielectric permittivity, ε_r.	9	14.6	10	3
N_C effective density (cm^{-3})	2.2×10^{18}	2.2×10^{18}	2.2×10^{19}	2.2×10^{18}
N_C effective density (cm^{-3})	1.8×10^{19}	1.8×10^{19}	1.8×10^{19}	1.8×10^{19}
Electron thermal velocity (cm/s)	1.8×10^{7}	1.8×10^{7}	1.0×10^{7}	1.0×10^{7}
Hole thermal velocity (cm/s)	1.0×10^{7}	1.0×10^{7}	1.0×10^{7}	1.0×10^{7}
Electron mobility, μ_n (cm^2/Vs)	20	60	100	$2x10^{-4}$
Hole mobility, μ_p (cm^2/Vs)	10	20	25	$2x10^{-4}$
Carrier density of the donor, N_D (cm^{-3})	1×10^{18}	-	1×10^{17}	-
N_A Acceptor density	-	1×10^{18}	-	2×10^{18}

1.2 Alignment of band structure

The varying of electron affinities of the buffer material and the absorber material affect the performance of the photovoltaic cell device (Sadanand et al., 2021). This is true even when the alignment of band structure for the transit of photogenerated carriers is not critical. Figure 2 depicts the resulting optimized band diagram.

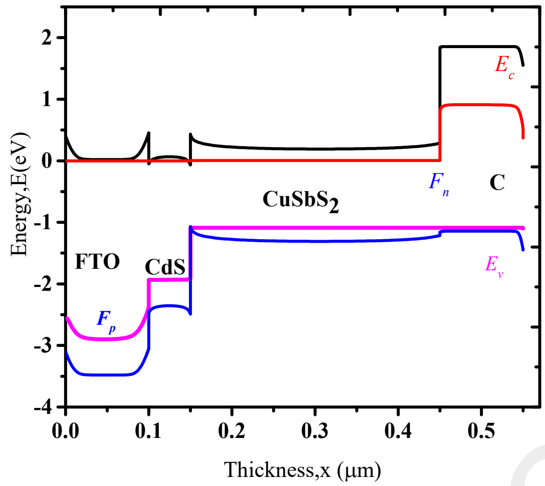

Fig.2 Energy band diagram

Where E_c, E_v, F_p and F_n are conduction energy, valence energy and Quasi-Femi energy for electron and hole respectively. The electron affinity and photoactive layer gives the nature of heterointerface band, (Meher et al., 2016). From the alignment there is a spike like conduction band offset at CdS implying inbuilt potential barrier to photogenerated electrons. Since the majority charge carriers recombine at the interface due to defects, V_{oc} drops when the forward bias is applied, making the conduction band offset at the CdS/$CuSbS_2$ interface the limiting factor.

2. Results and Discussion

2.1. *Impact of thickness variation of FTO.*

Müller et al., (2004) state that transparent conducting oxides (TCOs) are used as a front electrode and a backside reflector. By adjusting the FTO layer thickness, we were able to examine how it affected performance of copper antimony sulphide cell. Increasing fluorine doped tin oxide thicknesses from 100 nm to 600 nm while maintaining same values for the other layers led to a noticeable increment in Jsc, Voc, FF and photovoltaic cell efficiency, as shown in Figure.3. when FTO thickness increases, there is a smaller delta Voc and a smaller delta Jsc (from 28.28 to 28.19 mA/cm^2) as depicted in figure 3(a).

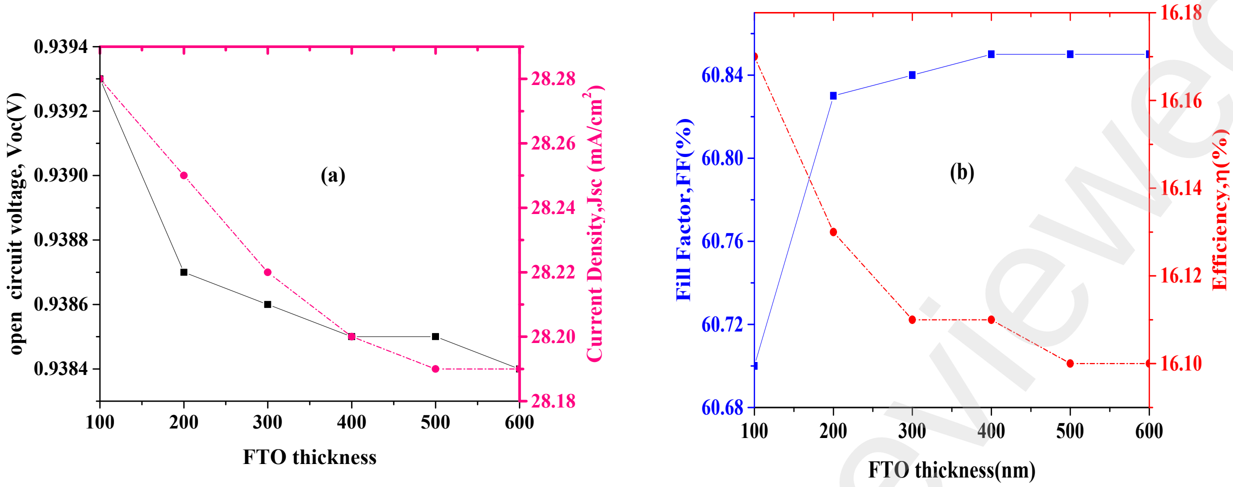

Fig3.Variation of (a) Voc and Jsc (b) FF and efficiency with FTO thickness.

Figure 3(b) shows that as thickness of FTO was increased from 100 nm to 600 nm, fill factor increases from 60.70% - 60.85%, but efficiency slightly decreases from 16.17% to 16.10%. From the above, the decrease in efficiency by a small margin (0.070) has no much significance on the solar cell. Increase in FTO thickness from 100 nm to 600 nm does not have a significant effect, the thicker the layer, the more the absorption of photons. Therefore, 100 nm thick FTO was considered for maximum output of open circuit voltage of the photovoltaic cell (Isoe et al., 2020).

2.2 Effect of CdS Thickness.

As the medium that carries the produced electrons from the absorber layer to the front contact and blocks the holes' path to the FTO electrode, CdS is crucial to the device's operation. Carbon was at 50 nm, FTO at 100 nm, and $CuSbS_2$ at 300 nm, while the thickness of cadmium sulphide ranged from 10 nm to 500 nm. From the simulation, both Voc and Jsc reduces with increase in CdS thickness as shown in fig.4(a), also the fill factor and efficiency decrease with the rise of electron transport layer thickness as shown in figure 4(b). The result implies that increase of thickness of ETL leads to charge recombination due to charges staying for long time at the layer hence recombining with oppositely charged particles through the interface with the photoactive layer. Also, the increase of CdS in the path of incident solar radiation may have decreased transmittance therefore the delivered photons to $CuSbS_2$ would have been less leading to low Voc. Due to the reduction in open circuit voltage, it also reduces efficiency and fill factor of the cell, this might be due to increment of series resistance as ETL thickness is increased. Therefore, the optimum ETL thickness is 50nm which gave the solar cell efficiency of 16.17%.

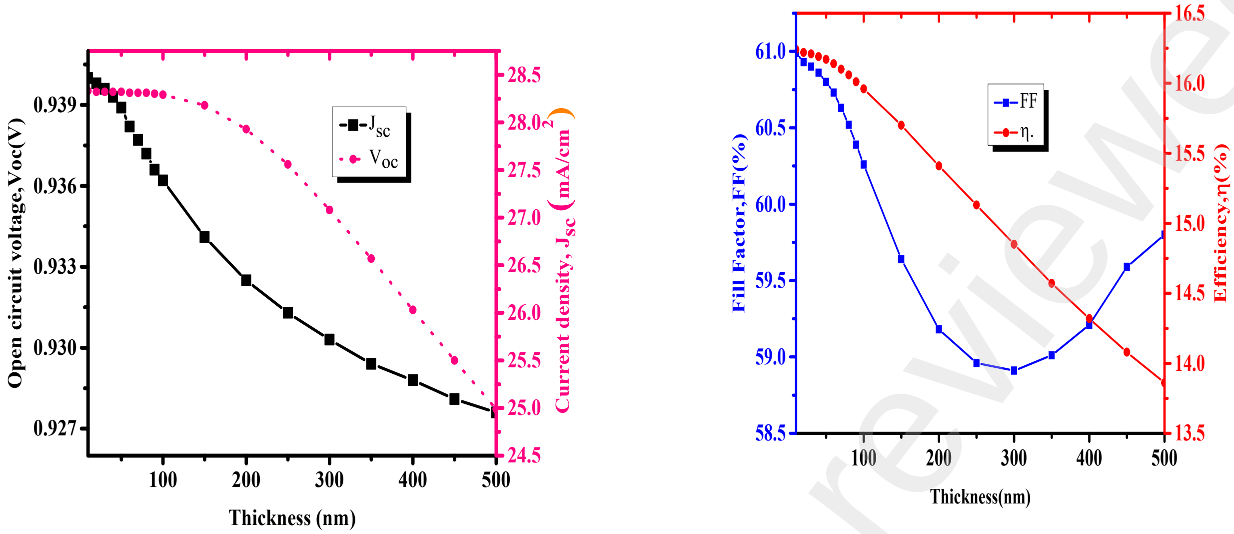

Fig 4(a)Variation of Voc and Jsc (b) FF and efficiency with CdS thickness.

2.3. Impact of thickness of a photoactive layer.

Since device efficiency is directly proportional to the absorber layer thickness, photovoltaic cell simulation was performed to examine the effect varying thickness of copper antimony sulphide photovoltaic cell characteristics such as Voc, Jsc, FF, and efficiency. To account for the requirement that the absorber layer be thicker than any other layer, the variation of thickness from 200 nm - 1200 nm while all other layer's characteristics were held constant (Sadanand et al., 2021). Fig 5(a) indicated that while thickness of $CuSbS_2$ increases from 100 - 1200 nm, the short-circuit current density (Jsc) also increases. This is because more radiation is absorbed, which causes a higher concentration of carriers. $CuSbS_2$ has a high absorption coefficient of 10^5 cm^{-1}, which is connected to the enhancement of Jsc (Nair & Nair, 2001). Recombination of charge carriers produced by the increment of absorber thickness arising from near the center of the $CuSbS_2$ layer reduces Voc when the diffusion length is greater than the absorber thickness, which is observed when the absorber depth of more than 700 nm. In addition, as thickness of copper antimony sulphide grows from 100 nm to 1200 nm, the effective bandgap of $CuSbS_2$ grows smaller, resulting in a lower open circuit voltage (Nalianya et al., 2021). The fill factor also falls, from 61.38 to 60.70%. This is due to the fact that the fill factor decreases as the absorber's thickness grows in direct proportion to the resistance imposed by the material (Bag et al., 2020). Due to increment of recombination and a drop on extraction rate of charge carriers, the efficiency marginally drops with high thickness of photoactive layer. As absorber grows thicker, more long-wavelength solar irradiation is soaked up, leading to more exciton creation and dissociation, which in turn leads to more electron-hole pairs and higher efficiency (Sadanand & Dwivedi, 2020). This means that a photovoltaic cell with an efficiency of 16.17% requires a photoactive layer thickness of exactly 300 nm.

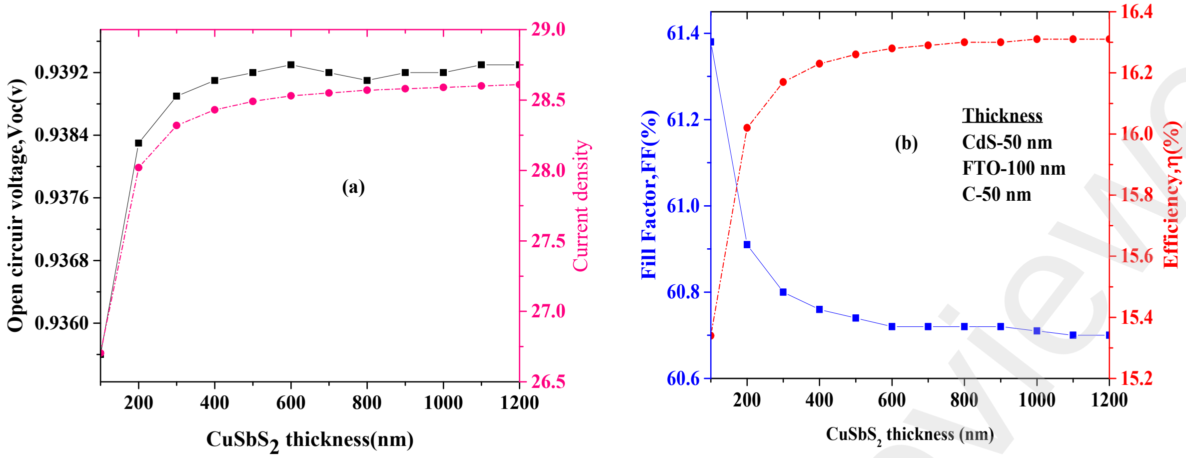

Fig 5(a)Variation of Voc and Jsc (b) FF and efficiency with $CuSbS_2$ thickness.

2.4 Effect of Carbon Thickness.

When electrons are blocked, holes are created, and carbon plays a part in transporting these holes and improving the device's performance. The variation of the thickness of carbon from 50 nm to 500 nm while CdS, $CuSbS_2$, and FTO were held constant at 50 nm, 300 nm, and 100 nm, respectively. Based on result, Fig. 6(a) illustrates how the Voc and Jsc depend on the thickness of carbon, whereas Figure 6(b) depicts how fill factor and cell efficiency depend on the thickness of carbon. As HTL thickness was increased, the fill factor and efficiency were decreased due to the decrease in irradiance and the increase in recombination of charge carriers.

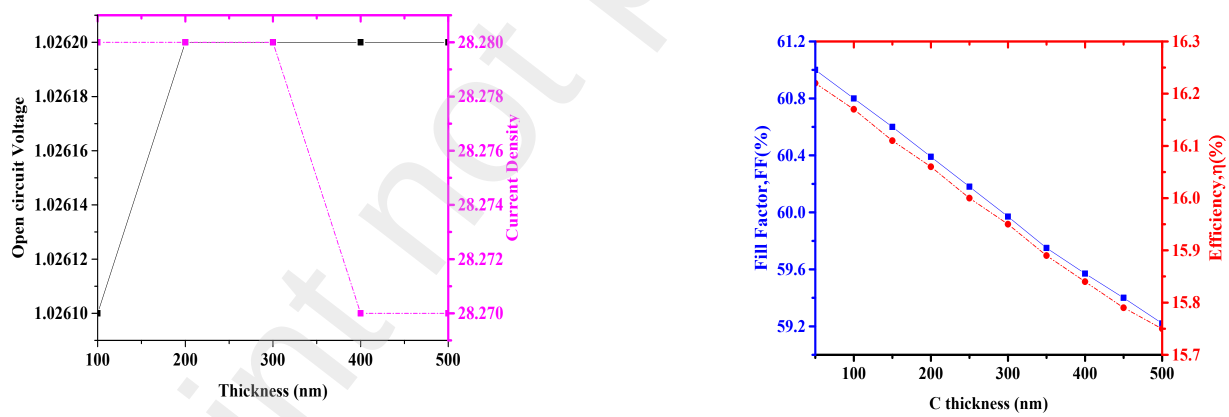

Fig 6(a)Variation of Voc and Jsc (b) FF and efficiency with C thickness.

2.5 Impact of dopant concentration of photoactive layers on solar cells parameters.

There is a correlation between the doping concentration of $CuSbS_2$ and its electrical properties, resulting to affecting efficiency of photovoltaic cells. Doping concentrations in the absorber layer were changed from 1 x 10^{14} cm^{-3} - 1 x 10^{18} cm^{-3}, with thickness of absorber layer held constant at 300 nm, to see how doing so affected the performance characteristics of the solar cells. Doping concentration data are presented in Fig. 7.

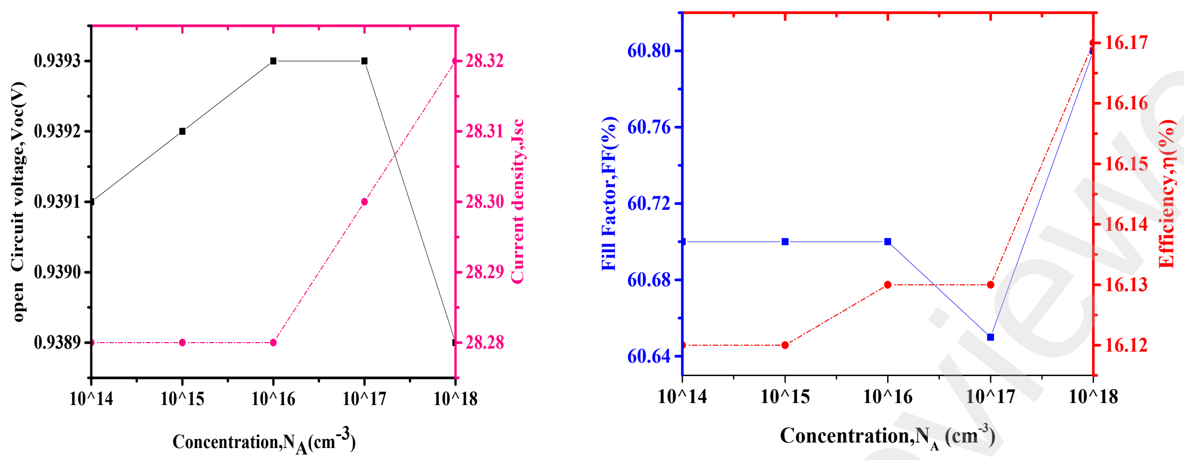

Fig 7(a)Variation of Voc and Jsc (b) FF and efficiency with dopant concentration.

Doping at 10^{18}cm^{-3}a, as illustrated in fig. 7 above, maximizes solar cell efficiency at over 16% while also producing a high current density. Although the fill factor decreased significantly at a doping concentration of 1x10^{17}cm^{-3} due to reduction of the electric field causing a rise in forward bias, Voc rose steadily with increasing concentration because charge carriers were efficiently transported, as in the work presented by (Nalianya et al., 2021b). In addition, it is seen that a higher concentration of dopant results in a higher fill factor and higher efficiency. This is because the number of majority carriers in the p-type region of doped copper antimony sulfide grows. As a result of increased auger recombination brought about by a high concentration, forward biasing increases.

2.6 The impact of defect density of photoactive layers on photovoltaic cells parameter.

Defect density of the photoactive layer was varied from 1x10^{8} to 1x10^{10}cm^{-3} while crosssectional area was maintained at 1x10^{-19} cm^{-2}. According to table 2, carrier recombination causes an increase in defect density, as a result shortens the carrier lifespan and shortens the length of diffusion, findings that are consistent with those published by (Devi et al., 2018). Due to decreased recombination, the diffusion length increases as the defect density decreases, and this is due to an increase in the carrier lifespan.

Table 2. Defect density and diffusion length

Parameter			
Defect density(cm^{-3})	10^{10}	10^{9}	10^{8}
Diffusion Length (nm)	719.53	2275.0	7195.3

2.7J-V characteristics of the optimized parameters.

Copper antimony sulphide has the potential to be used as an absorber material in photovoltaic applications, as demonstrated by its open circuit voltage of 0.9388 V, short circuit current density of 28.31mA/cm^{-2}, fill factor of 60.8%, and efficiency of 16.17% when carbon is used as the hole transport layer. The J-V characteristic of optimized film without carbon depicted the Voc of 0.2419, Jsc of 28.22, fill factor of 44.47, and efficiency of 3.4%.

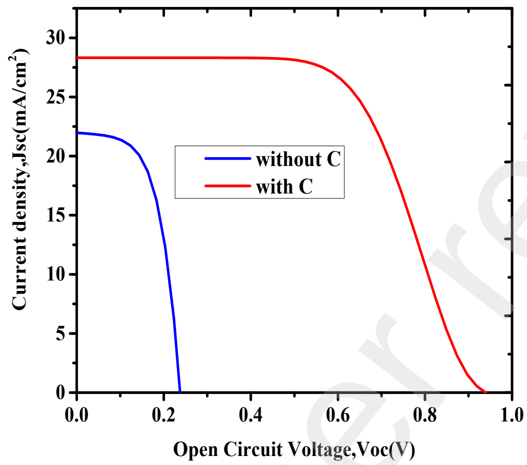

Fig.8 J-V curve of optimized solar cell with and without HTL.

3. Conclusion

SCAPS-1D software was used to simulate a $CuSbS_2$ solar cell with a design of glass/SnO_2: F/CdS/$CuSb_2$/C/Au. The effects of varying the thicknesses of FTO, CdS, $CuSbS_2$, and C on device performance were studied. According to the simulation results, there is little correlation between the thickness of the CdS absorber and the device's operations, and a photoactive thickness of 300 nm to 400 nm is optimal for improved solar cell operations. Additionally, the modeling results showed that a superior solar cell parameter was achieved with a layer thickness of 100 nm for FTO, 50 nm for CdS, 300 nm for $CuSbS_2$, and 100 nm for C. The efficiency of the photovoltaic cell increased from 16.12% to 16.17% as dopant concentration was varied, and the diffusion length decreased with increasing defect density, indicating less recombination process. Therefore, the optimized solar cell gave efficiency of 16.17% suggesting good material for fabrication for photovoltaic applications.

Acknowledgments

We give our sincere gratitude to Prof. Marc Burgelman and his staff at the University of Gent, Belgium, whole heartedly distributing SCAPS-1D simulator. We also appreciate the Computational and Theoretical Physics (CTheP), Masinde Muliro University of Science and Technology group for the computation facilities.

References

Andersson, Johansson, N., Johansson P, Yu, N, Lupo, D, & Salaneck, W. R. (1998). Fluorine tin oxide as an alternative to indium tin oxide in polymer LEDs. *Advanced Materials*, *10*(11), 859–863.

Banu, S., Cho, Y., Kim, K., Ahn, S. K., Gwak, J., & Cho, A. (2019). Phase transition behavior and defect analysis of CuSbS2 thin films for photovoltaic application prepared by hybrid inks. *Solar Energy*, *188*, 1209–1220. https://doi.org/10.1016/j.solener.2019.07.019

Benami, A. (2019). Effect of CZTS Parameters on Photovoltaic Solar Cell from Numerical Simulation. *Journal of Energy and Power Engineering*, *13*. https://doi.org/10.17265/1934-8975/2019.01.003

Burgelman, M., Nollet, P., & Degrave, S. (2000). Modeling polycrystalline semiconductor solar cell. *Thin Solid Films*, *361*, 527–532. https://doi.org/10.1016/S0040-6090(99)00825-1

Ghorbani, E. (2020). On efficiency of earth-abundant chalcogenide photovoltaic materials buffered with CdS: the limiting effect of band alignment. *Journal of Physics: Energy*, *2*(2), 025002. https://doi.org/10.1088/2515-7655/ab6942

Isoe, W., Mageto, M., Maghanga, C. M., Mwamburi, M., Odari, B., & Awino, C. (2020). Thickness Dependence of Window Layer on CH 3 NH 3 PbI 3-X Cl X Perovskite Solar Cell. *International Journal of Photoenergy*, *2020*, 1–7. https://doi.org/10.1155/2020/8877744

Macías, C., Lugo, S., Benítez, Á., López, I., Kharissov, B., Vázquez, A., & Peña, Y. (2017). Thin film solar cell based on CuSbS2 absorber prepared by chemical bath deposition (CBD). *Materials Research Bulletin*, *87*, 161–166. https://doi.org/10.1016/j.materresbull.2016.11.028

Meher, S. R., Balakrishnan, L., & Alex, Z. C. (2016). Analysis of Cu2ZnSnS4/CdS based photovoltaic cell: A numerical simulation approach. *Superlattices and Microstructures*, *100*, 703–722. https://doi.org/10.1016/j.spmi.2016.10.028

Nalianya, M. A., Awino, C., Barasa, H., Odari, V., Gaitho, F., Omogo, B., & Mageto, M. (2021). Numerical study of lead free CsSn0.5Ge0.5I3 perovskite solar cell by SCAPS-1D. *Optik*, *248*, 168060. https://doi.org/10.1016/j.ijleo.2021.168060

Olopade, M., Adewoyin, A., Chendo, M., & Bolaji, A. (2018, December). *The Study of Some Materials as Buffer Layer in Copper Antimony Sulphide (CuSbS 2) Solar Cell Using SCAPS 1-D*.

Perniu, D., Duta, A., & Schoonman, J. (2006). Defect Chemistry of Cusbs2. *2006 International Semiconductor Conference*, *2*, 245–248. https://doi.org/10.1109/SMICND.2006.283988

Sadanand, & Dwivedi, D. K. (2020). Modeling of CZTSSe solar photovoltaic cell for window layer optimization. *Optik*, *222*, 165407. https://doi.org/10.1016/j.ijleo.2020.165407

Wang, L., Zhao, X., Yang, Z., Ng, B., Jiang, L., Lai, Y., & Jia, M. (2021). CuSbS2 Solar Cells Using CdS, In2S3 and the In/Cd-based Hybrid Buffers. *Journal of Electronic Materials*, *50*. https://doi.org/10.1007/s11664-021-08815-w

Willian de Souza Lucas, F., Peng, H., Johnston, S., Dippo, P. C., Lany, S., Mascaro, L. H., & Zakutayev, A. (2017). Characterization of defects in copper antimony disulfide. *J. Mater. Chem. A*, *5*(41), 21986–21993. https://doi.org/10.1039/C7TA07012H

Xu, Y., Ye, Q., Chen, W., Pan, X., Hu, L., Yang, S., Hayat, T., Alsaedi, A., Zhu, J., & Dai, S. (2018). Solution-processed CuSbS2 solar cells based on metal–organic molecular solution precursors. *Journal of Materials Science*, *53*. https://doi.org/10.1007/s10853-017-1663-8